

Quantum-critical pairing with varying exponents

Eun-Gook Moon

Department of Physics, Harvard University, Cambridge MA 02138

Andrey Chubukov

Department of Physics, University of Wisconsin, Madison, Wisconsin 53706

(Dated: November 24, 2018)

We analysed the onset temperature T_p for the pairing in cuprate superconductors at small doping, when tendency towards antiferromagnetism is strong. We considered the model of Moon and Sachdev (MS), which assumes that electron and hole pockets survive in a paramagnetic phase. Within this model, the pairing between fermions is mediated by a gauge boson, whose propagator remains massless in a paramagnet. We related the MS model to a generic γ -model of quantum-critical pairing with the pairing kernel $\lambda(\Omega_n) \propto 1/\Omega_n^\gamma$. We showed that, over some range of parameters, the MS model is equivalent to $\gamma = 1/3$ -model ($\lambda(\Omega) \propto \Omega^{-1/3}$). We found, however, that the parameter range where this analogy works is bounded on both ends. At larger deviations from a magnetic phase, the MS model becomes equivalent to γ model with varying $\gamma > 1/3$, whose value depends on the distance to a magnetic transition and approaches $\gamma = 1$ deep in a paramagnetic phase. Very near the transition, the MS model becomes equivalent to γ model with varying $\gamma < 1/3$. Right at the magnetic QCP, the MS model is equivalent to the model with $\lambda(\Omega_n) \propto \log \Omega_n$, which is the model for color superconductivity. Using this analogy, we verified the formula for T_c derived for color superconductivity.

PACS numbers:

I. INTRODUCTION

A quest for understanding of the phase diagram of cuprates and other strongly correlated electron systems generated strong interest to the pairing problem near a quantum critical point (QCP). In distinction to a conventional BCS/Eliashberg theory, in which pairing is mediated by an interaction which can be approximated by a constant at small frequencies, quantum-critical pairing is mediated by gapless, dynamical collective modes¹. In most cases, only a particular charge or spin mode becomes gapless at criticality, and the same interaction that gives rise to pairing also accounts for the fermionic self-energy. In systems with $d \leq 3$, $\partial\Sigma(k, \omega)/\partial\omega$ diverges at $\omega \rightarrow 0$, i.e., interaction with a gapless collective modes destroys fermionic coherence either at particular hot spots¹, if the emerging order parameter has a finite momentum q , or along the whole Fermi surface (FS) if the ordering is with $q = 0$ (Ref.³). Then, in another distinction to a conventional BCS/Eliashberg theory, the pairing involves incoherent fermions.

The self-energy at a QCP generally behaves as $\omega_0^\gamma \omega^{1-\gamma}$, where $\gamma > 0$, while the effective dynamic pairing interaction (the analog of phonon $\alpha^2(\Omega)F(\Omega)$) scales $\lambda(\Omega) \propto (\Omega_0/\Omega)^\gamma$. The kernel $K(\omega, \omega')$ of the equation for the pairing vertex $\Phi(\omega) = \pi T \sum_{\omega'} K(\omega, \omega') \Phi(\omega')$ then scales as

$$K(\omega, \omega') = \frac{\lambda(\omega - \omega')}{|\Sigma(\omega')|} \propto \frac{1}{|\omega - \omega'|^\gamma |\omega'|^{1-\gamma}}. \quad (1)$$

It has the same scaling dimension -1 as in BCS theory, which corresponds to $\gamma = 0$. However, in distinction to BCS theory, where the kernel is $1/|\omega'|$, the kernel $K(\omega - \omega')$ for $\gamma > 0$ depends on both external and

internal energy, and the onset temperature for the pairing T_p has to be obtained by solving integral equation for the frequency-dependent pairing vertex $\Phi(\omega)$ (we label this temperature as T_p to distinguish it from the actual superconducting T_c which is generally lower because of phase and amplitude fluctuations of $\Phi(\omega)$). The frequency dependence of the vertex by itself is not unique to a QCP and is present already in the Eliashberg theory of conventional superconductors¹³. However, as we said, in conventional cases, the frequency dependence is relevant at high frequencies, while the low-frequency sector can still be treated within BCS theory. The new element of quantum-critical pairing is that non-trivial frequency dependence of the pairing vertex extends down to $\omega = 0$ leaving no space for the BCS regime.

To shorten the notations, below we label the model of QC pairing mediated by $\lambda(\Omega) \propto 1/|\Omega|^\gamma$ as the γ -model. Examples of γ -models, include 2D pairing by ferromagnetic or antiferromagnetic spin fluctuations ($\gamma \approx 1/3$ and $\gamma \approx 1/2$, respectively^{1-3,20}), and 3D pairing by gapless charge or spin fluctuations ($\gamma = 0+$, implying that $\lambda(\Omega) \sim \log \Omega$ and $\Sigma(\omega) \sim \omega \log \omega$, Ref.^{8,19}). Another example of $\gamma = 0+$ behavior is color superconductivity of quarks mediated by gluon exchange⁷. The $\gamma = 1/3$ model describes the pairing of composite fermions at $\nu = 1/2$ Landau level.⁹ A similar problem with momentum integrals instead of frequency integrals have been considered in Ref. 10.

The solutions of the pairing problem in these systems differ in details but have one key feature in common – T_p monotonically increases upon approaching a QCP from a disordered side. At a QCP, $T_p = \Omega_0 f(\gamma)$, where $f(\gamma)$ is a smooth function, which decreases when γ increases.

Recently, Moon and Sachdev (MS) considered⁵ an

other example of QC pairing – the pairing of fermions in the presence of spin-density-wave (SDW) background, which can be either in the form of long-range SDW order, or SDW precursors. MS argued that the phase with SDW precursors is an algebraic charge-liquid in which fermions still possess the same pocket FS as in the SDW phase¹⁵. They found that the model remains critical away from critical point because of the presence of gapless gauge fluctuations, and T_p actually increases as the system moves away from a QCP into a charge-liquid phase. This trend is opposite compared to a magnetically-mediated pairing without SDW precursors. This result is quite important for the understanding of the pairing in the cuprates as it shows that the onset temperature of the pairing instability does form a dome centered around a doping at which the system develops SDW precursors.^{6,15,21} In the region where SDW precursors are not yet formed, there is a large Fermi surface, and T_p increases as doping decreases and the system comes closer to a magnetic instability. Once SDW precursors are formed above T_p , the trend changes, and T_p passes through a maximum and begins decreasing with decreasing doping.

The reason for the opposite behavior of T_p in the presence of SDW precursors is the suppression of the d -wave pairing vertex. In the ordered SDW state, the interaction between fermions mediated by Goldstone bosons is dressed up by SDW coherence factors and vanishes at the ordering momentum by Adler principle¹⁸. In the disordered phase, there are no such requirement, but the vertex is still suppressed as long as the system has SDW precursors. As the system moves away from a QCP, SDW precursors weaken, the pairing interaction gradually increases towards its value without precursors, and T_p increases.

The goal of this communication is to relate the pairing problem in the presence of SDW precursors with earlier studies of the pairing within the γ model. We argue that the MS model belongs to the class of γ -models, however the relation between the two is rather non-trivial. First, the pairing in the MS model remains quantum-critical even away from the QCP, when spin excitations acquire a finite mass m at $T = 0$, i.e., the MS model away from the QCP is equivalent to a γ -model right at criticality. Second, we show that the MS model at different deviations from the QCP is equivalent to γ -models with different γ , ranging from $\gamma = 0+$ right at the QCP to $\gamma = 1$ deep into the magnetically-disordered phase (but still with SDW precursors). Third, the scale Ω_0 in $\lambda(\Omega) = (\Omega_0/|\Omega|)^\gamma$ also becomes γ -dependent and increases with increasing γ . This is the key reason why $T_p \propto \Omega_0$ increases into the disordered state.

We also consider in more detail the pairing problem right at the QCP. We find that at this point, the pairing interaction at small frequencies is $\lambda(\Omega) = g \log(\Omega_0/|\Omega|)$ and the fermionic self-energy $\Sigma(\omega) = g\omega \log(\Omega_0/|\omega|)$, are logarithmical and depend separately on the cutoff scale Ω_0 and on the dimensionless coupling constant g . This

separate dependence is unique to the logarithmical form of the pairing interaction, for any power-law form of $\lambda(\Omega) = (\Omega_0/\Omega)^\gamma$, the coupling g is incorporated into ω_0 . At frequencies $\Omega > \Omega_0$, $\lambda(\Omega)$ decays faster than the logarithm, eventually as $1/\Omega$. As we said, the same logarithmical form of the pairing vertex appears in the problem of color superconductivity. For color superconductivity, Son obtained at weak coupling $T_p \propto \omega_0 e^{-\pi/(2\sqrt{g})}$ [Ref.⁷]. The result is similar to the BCS formula, but the dependence on the coupling is \sqrt{g} rather than $1/g$. Son's result was confirmed in subsequent analytical studies, but, to the best of our knowledge, it has not been verified by actually solving the linearized gap equation for the case when the interaction is logarithmical at small frequencies and decays as a power of $1/\Omega$ at larger frequencies. We solved this equation for our $\lambda(\Omega)$, obtained T_p , and found excellent agreement with $e^{-\pi/(2\sqrt{g})}$ behavior.

The paper is organized as follows. In Sec. II we briefly review (i) Eliashberg-type theory for the pairing induced by frequency dependent pairing kernel $K(\Omega)$, (ii) the γ -model with no SDW precursors, and (iii) the MS model for the pairing in the presence of SDW precursors. In Sec. III we show that the MS model reduces to the set of γ -models with varying γ , which gradually increases from $\gamma = 0+$ as one moves away from the QCP. We argue that γ remains $1/3$ over some range of deviations from the QCP, but this range is quite narrow. In Sec. IV we consider in more detail the MS model at the QCP and show that at this point it is equivalent to the γ model at $\gamma = 0+$ which in turn is equivalent to the model for color superconductivity. We present the numerical solution for the pairing vertex, and show that $\log T_c/E_F$ scales as $1/\sqrt{g}$. Sec. V presents our conclusions.

II. REVIEW OF THE MODELS

A. Eliashberg theory

Throughout the paper we assume that the pairing problem can be treated within Eliashberg-type theory, i.e., assume that the pairing kernel and the fermionic self-energy have singular frequency dependence but no substantial momentum dependence. The justifications for neglecting the momentum dependence are to some extent problem-specific, but generally are due to the fact that collective bosons are Landau overdamped what makes them slow modes compared to electrons.

Within Eliashberg theory, the fermionic Green's function in Nambu spinor notations is given by

$$\begin{aligned} \hat{\Sigma}(\omega_n) &= i\Sigma(\omega_n)\hat{\tau}_0 + \Phi(\omega_n)\hat{\tau}_1 \\ \hat{G}^{-1}(\epsilon_k, \omega_n) &= i(\omega_n + \Sigma(\omega_n))\hat{\tau}_0 - \epsilon_k\hat{\tau}_3 - \Phi(\omega_n)\hat{\tau}_1 \end{aligned} \quad (2)$$

where $\hat{G}^{-1} = \hat{G}_0^{-1} + \hat{\Sigma}$, $\hat{\tau}$ are the Pauli matrices in the particle-hole space, ϵ_k is the fermionic dispersion in the normal state, $\Phi(\omega_n)$ is a pairing vertex, and $\Sigma(\omega_n)$ is a

conventional (non-Nambu) self-energy. The Nambu self-energy $\hat{\Sigma}(\omega_n)$ in turn is expressed via the full Green's function as

$$\begin{aligned}\hat{\Sigma}(i\omega_n) &= -T \sum_{\omega_m} \lambda(\omega_m - \omega_n) \int d\epsilon_k \hat{G}(\epsilon_k, \omega_m) \\ &= i\Sigma(\omega_n)\hat{\tau}_0 + \Phi(\omega_n)\hat{\tau}_1\end{aligned}$$

The full set of Eliashberg equations is obtained by matching the coefficients of the Pauli matrices term by term:

$$\begin{aligned}\Sigma(\omega_n) &= \pi T \sum_{\omega_m} \lambda(\omega_m - \omega_n) \frac{\omega_m + \Sigma(\omega_m)}{\sqrt{(\omega_m + \Sigma(\omega_m))^2 + \Phi^2(\omega_m)}} \\ \Phi(\omega_n) &= \pi T \sum_{\omega_m} \lambda(\omega_m - \omega_n) \frac{\Phi(\omega_m)}{\sqrt{(\omega_m + \Sigma(\omega_m))^2 + \Phi^2(\omega_m)}}\end{aligned}\quad (3)$$

This set of two non-linear self-consistent integral equations can be reduced to just one integral equation by introducing the inverse quasiparticle renormalization factor $Z(\omega_n) = 1 + \Sigma(\omega_n)/\omega_n$ and the pairing gap $\Delta(\omega_n) = \Phi(\omega_n)/Z(\omega_n)$. The equation for $\Delta(\omega_n)$ then decouples from the equation on $Z(\omega_n)$ and takes the form

$$\Delta(\omega_n) = \pi T \sum_{\omega_m} \frac{\lambda(\omega_m - \omega_n)}{\sqrt{\omega_m^2 + \Delta^2(\omega_m)}} \left(\Delta(\omega_m) - \Delta(\omega_n) \frac{\omega_m}{\omega_n} \right)\quad (4)$$

The inverse quasiparticle renormalization factor $Z(\omega_n)$ is then obtained by substituting the result for $\Delta(\omega_m)$ into

$$\omega_n Z(\omega_n) = \omega_n + \pi T \sum_{\omega_m} \lambda(\omega_m - \omega_n) \frac{\omega_m}{\sqrt{\omega_m^2 + \Delta^2(\omega_m)}}\quad (5)$$

To obtain T_p we will need to set $\Phi, \Delta \rightarrow 0$ and solve the linearized equation either for the pairing vertex or the pairing gap. Both are non-self-consistent equations in this limit because at Φ can be safely dropped from the expression for $\Sigma(\omega_n)$ which becomes:

$$\Sigma(\omega_n) = \pi T \sum_{\omega_m} \lambda(\omega_m - \omega_n) \text{sign}(\omega_m), \quad Z(\omega_n) = 1 + \frac{\Sigma(\omega_n)}{\omega_n}\quad (6)$$

It is more straightforward to analyze the linearized equation for the pairing vertex $\Phi(\omega_n)$:

$$\Phi(\omega_n) = \pi T \sum_{\omega_m} K(\omega_n, \omega_m) \Phi(\omega_m),\quad (7)$$

where the kernel is

$$K(\omega_n, \omega_m) = \frac{\lambda(\omega_m - \omega_n)}{|\omega_m| Z(\omega_m)}\quad (8)$$

B. the γ -model

We use the term γ -model as abbreviation for a critical model in which the pairing is mediated by a gapless

boson, and $\lambda(\omega_n - \omega_m)$ has a power-law form

$$\lambda(\Omega) = \left(\frac{\Omega_0}{|\Omega|} \right)^\gamma\quad (9)$$

We assume in this work that $\gamma < 1$. The analysis of the γ -models with $\gamma \geq 1$ is more involved (and more non-trivial), but we will only need $\gamma < 1$ for comparisons with the MS theory.

To put this into perspective, we remind that in BCS theory $\lambda(\Omega_n)$ is a constant up to a cutoff scale above which it is set to zero. In Eliashberg theory for non-critical superconductors $\lambda(\Omega_n)$ has some frequency dependence but still reduces to a constant at small frequencies. In this situation, the pairing problem differs from BCS problem quantitatively but not qualitatively. In Eq. (9), however, the pairing interaction preserve singular frequency dependence down to $\Omega = 0$. This makes the pairing problem in the γ -model qualitatively different from BCS problem.

The divergence of $\lambda(\Omega_m)$ at zero bosonic Matsubara frequency $\Omega = 0$ is by itself not relevant for the pairing as can be straightforwardly seen from Eq. (4) for $\Delta(\omega_m)$: the term with $m = n$ in the r.h.s. of this equation vanishes. This vanishing is essentially the manifestation of the Anderson theorem for a dirty s -wave superconductors because the scattering with zero frequency transfer is formally analogous to impurity scattering^{2,22,23}. The recipe then is to eliminate the term with zero bosonic Matsubara frequency from the frequency sums, what we will do.

The fermionic self-energy for such $\lambda(\Omega)$ has the form

$$\Sigma(\omega_n) = \omega_n \left(\frac{\Omega_0}{|\omega_n|} \right)^\gamma S(\gamma, n)\quad (10)$$

where

$$S(\gamma, m) = \frac{1}{(m + 1/2)^{1-\gamma}} [\zeta(\gamma) - \zeta(\gamma, m + 1)]\quad (11)$$

where $\zeta(\gamma)$ and $\zeta(\gamma, m + 1)$ are Riemann zeta function and generalized Riemann zeta function, respectively. We plot $S(\gamma, m)$ in Fig. 1. At large m , $S(\gamma, m)$ approaches $1/(1 - \gamma)$, and the self-energy becomes $\Sigma(\omega_n) = \omega_n^{1-\gamma} (\Omega_0^\gamma / (1 - \gamma))$ (this limiting form is reproduced if the summation over ω_m is replaced by the integration).

The rate with which $S(\gamma, m)$ approaches $1/(1 - \gamma)$ by itself depends on γ and slows down when γ approaches one. For $1 - \gamma \ll 1$, $S(\gamma, m)$ at large m behaves as $S(\gamma, m) \approx (1 - m^{-(1-\gamma)})/(1 - \gamma)$ and becomes $\log m$ at $\gamma = 1$.

Substituting the self-energy into the equation for $\Phi(\omega_m)$ and rescaling the temperature by Ω_0 we find, instead of (7),

$$\begin{aligned}\Phi(\omega_n) &= \sum_{\omega_m} \frac{\Phi(\omega_m)}{|2m + 1|} \times \\ &= \frac{1}{|S(\gamma, m) \left(\frac{|m-n|}{|m+1/2|} \right)^\gamma + (2\pi|m-n|)^\gamma \left(\frac{T}{\Omega_0} \right)^\gamma}.\end{aligned}\quad (12)$$

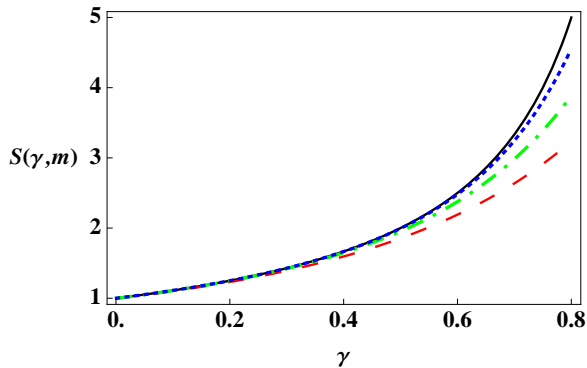


FIG. 1: Generalized Riemann-zeta function, $S(\gamma, m)$. The dashed (red), dot-dashed (green) and dotted (blue) lines correspond to $m = 100, 1000, 10000$. The black thick line is the asymptotic function $1/(1 - \gamma)$ valid at large m (see the text).

It is a priori not guaranteed that this equation has a solution at some T_p , but, if it does, T_p obviously scales as

$$T_p = \Omega_0 f(\gamma) \quad (13)$$

Eq (12) has been analyzed both analytically and numerically^{2,8-10,12,19}, and the result is that (i) the solution exists, and (ii) $f(\gamma)$ monotonically decreases with increasing γ , and remains finite at $\gamma = 1$, where $f(1) = 0.254$ (Ref.8).

C. the MS model

The MS model⁵ describes a phase transition between an SDW state and a magnetically disordered, algebraic charge liquid which still preserves electron pockets near $(0, \pi)$ and symmetry related points in the Brillouin zone. The model is two-dimensional and involves non-relativistic fermions with small FS, relativistic bosons which describe antiferromagnetic magnons, and a gauge field which couples bosonic and fermionic fields. There are two non-relativistic fermions (two FSs), with the action

$$\mathcal{L}_g = g_{\pm}^{\dagger} \left[\partial_{\tau} - \frac{\nabla^2}{2m^*} - \mu \right] g_{\pm}. \quad (14)$$

where m^* is a fermionic mass, and the chemical potential μ is chosen to fix the Fermi momentum k_F .

The action of a relativistic boson (an antiferromagnetic magnon) is

$$\mathcal{L}_z = \sum_{\alpha=1}^N \left(|\partial_{\tau} z_{\alpha}|^2 + v^2 |\nabla z_{\alpha}|^2 + m^2 |z_{\alpha}|^2 \right) \quad (15)$$

where m is the mass of a magnon

$$m = 2T \ln \left(\frac{e^{\frac{2\pi m^* v^2 \alpha_2}{T}} + \sqrt{4 + e^{\frac{4\pi m^* v^2 \alpha_2}{T}}}}{2} \right) \quad (16)$$

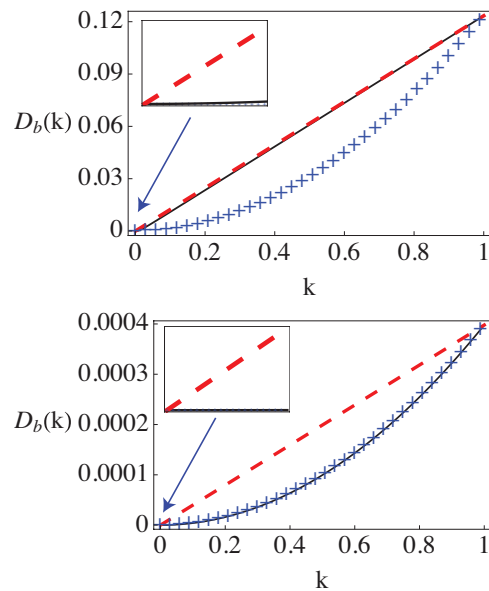


FIG. 2: The momentum dependence of $D_b(k)$ at zero temperature (black line) very near the QCP (top panel, $m = 0.01$) and far away from the QCP (lower panel, $m = 100$) k is in units of $2k_F$ and $D_b(k)$ is in units of $m^* v^2$ with $\alpha_1 = 0.5$. The thin-dashed line (Red) and the thin-dotted line (Blue) show linear and quadratic behavior, respectively. At the smallest k , $D_b(k)$ is quadratic for all $m > 0$ (see inserts), but for small m $D_b(k)$ rapidly crosses over to the linear behavior. For large m , the quadratic dependence survives up to maximal $k = 2k_F$. Note that the magnitude of $D_b(k)$ far away from the critical point is much smaller than near the QCP.

and the parameter α_2 measures the distance to a QCP (we use the same notations as in⁵). For $\alpha_2 < 0$ and $T = 0$, the system is in the ordered SDW phase ($m = 0$), for $\alpha_2 > 2$ and $T = 0$, the system is in the disordered phase ($m > 0$). At $T > 0$, there is no long-range order, and $m > 0$ for all α_2 , although for $\alpha_2 < 0$ it is exponentially small.

The gauge field couples bosonic and fermionic fields via minimal coupling ($\partial_{\mu} \rightarrow \partial_{\mu} \pm iA_{\mu}$). The two fermions (g_{\pm}) have opposite gauge charges, and gauge-field induced coupling between fermions and magnons is attractive and give rise to pairing. Both longitudinal and transverse parts of the interaction contribute to the pairing, but non-trivial physics comes from the interaction mediated by a transverse boson. For simplicity, we only consider transverse interaction.

The form of the transverse propagator of the gauge field $\chi_{tr}(k, \Omega_n)$ is obtained by combining the Landau damping term coming from fermions with the static part coming from magnons. MS found, for the physical case of $N = 2$ bosonic spinors,

$$\chi_{tr}(k, \Omega_n) = \left(\delta_{ij} - \frac{k_i k_j}{k^2} \right) \frac{1}{2D_b(k) + k_F |\Omega_n| / (\pi k)} \quad (17)$$

where

$$D_b(k) = \frac{v^2 k^2}{8\pi} \int_0^1 dx \frac{1}{\sqrt{m^2 + v^2 k^2 x(1-x)}} \times \coth\left(\frac{\sqrt{m^2 + v^2 k^2 x(1-x)}}{2T}\right). \quad (18)$$

In Fig. 2 we plot $D_b(k)$ at $T = 0$ near and far away from a critical point. At the smallest k , $D_b(k)$ scales as k^2 for any $m > 0$. For large m , this behavior holds up to $k \sim k_F$, but at small m , the k^2 dependence only holds for the smallest k crosses over to $D_b(k) \propto k$ at $vk \geq m$.

The frequency-dependent pairing interaction $\lambda(\Omega_n)$ is obtained in the usual way, by iterating the gauge field propagator $\chi_{tr}(k, \Omega_n)$ in the direction along the FS:

$$\lambda(\Omega_n) = \frac{\alpha_1 v}{2\pi^2} \int_0^{2k_F} dk \frac{\sqrt{1 - (k/2k_F)^2}}{2D_b(k) + k_F |\Omega_n| / (\pi k)} \quad (19)$$

where, following MS, we introduced another dimensionless parameter

$$\alpha_1 = \frac{k_F}{m^* v} \quad (20)$$

We will see that it plays the role of the dimensionless coupling.

Because $D_b(k)$ interpolates between k and k^2 dependences, the momentum integral in (20) diverges at $\Omega_n = 0$ no matter whether the system is at the QCP or away from the QCP (i.e., whether $m = 0$ or $m > 0$). This implies that the pairing in the MS model remains quantum-critical even when the system moves away from the actual critical point where SDW order emerges. Alternatively speaking, away from the QCP, magnetic excitations acquire a mass but the pairing gauge boson remains massless.

III. THE MS MODEL AS THE γ MODEL WITH VARYING EXPONENT γ

As the pairing is generally a low-temperature/low-frequency phenomenon, it is instructive to analyze first the form of $\lambda(\Omega_n)$ in the MS model, Eq. (19), at $T = 0$ and in the limit of small Ω_n . Suppose that the system is in the paramagnetic phase, where m tends to a constant at $T = 0$. Using (16), we obtain at $T = 0$, $m = 4\pi m^* v^2 \alpha_2 = 4\pi k_F v \alpha_2 / \alpha_1$. For small Ω_n the momentum integral in (19) is determined by k for which $D_b(k)k/k_F \sim |\Omega_n|$. These typical k are small when Ω_n are small. Substituting the small k expansion of $D_b(k) = v^2 k^2 / (8\pi m)$ (see Eq. (18)) into (19) we obtain

$$\lambda(\Omega_n) = \left(\frac{\Omega_0^{\gamma=1/3}}{|\Omega|} \right)^{1/3} \quad (21)$$

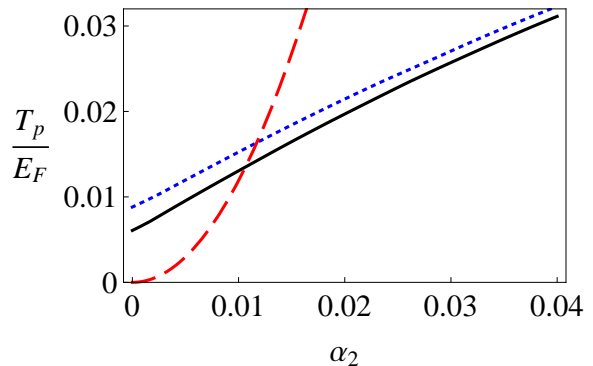


FIG. 3: The actual critical temperature T_p in the MS model with $\alpha_1 = 0.65$ (the black line) and $\alpha_1 \sim 0.75$ (the dotted blue line) (from Ref.⁵) and $T_p^{\gamma=1/3}$ from Eq. (24) (the dashed red line) Although the trend is the same – both the actual T_p and $T_p^{\gamma=1/3}$ increase with increasing α_2 , the functional forms are quite different. The two functions just cross at $\alpha_2 \sim 0.01$. Besides, the actual T_p does depend on α_1 , particularly for small α_2 , while $T_p^{\gamma=1/3}$ is independent on α_1 (see the text).

where

$$\Omega_0^{\gamma=1/3} = \frac{512\pi^2}{81\sqrt{3}} E_F \alpha_2^2 \quad (22)$$

and $E_F = k_F^2 / (2m^*)$. The corresponding self-energy is

$$\Sigma(\omega_m) = \frac{3}{2} \omega_m^{2/3} (\Omega_0^{\gamma=1/3})^{1/3}. \quad (23)$$

This $\lambda(\Omega_m)$ is the same as in the γ -model with $\gamma = 1/3$. The onset temperature for the pairing in the “1/3” model has been calculated in Refs.^{9,12} and is $T_p \approx 3.31 \Omega_0^{\gamma=1/3}$. Combing this result with Eq. (22), we obtain

$$T_p = T_p^{\gamma=1/3} \approx 119 E_F \alpha_2^2 \quad (24)$$

Observe that $T_p^{\gamma=1/3}$ depends on α_1 only via E_F .

Moon and Sachdev obtained T_p in the MS model numerically, using the full forms of $D_b(k)$ and $m(T)$. In Fig. 3 we compare their result with Eq. (24). We see that while the trend is the same – T_p increases with increasing α_2 , the functional forms of the actual T_p and $T_p^{\gamma=1/3}$ are very different, and Eq. (24) agrees with the numerical result for T_p only in a tiny range of α_2 near $\alpha_2 \sim 0.01$. Besides, T_p/E_F obtained numerically does depend on α_1 , in distinction to Eq. (24).

We looked into this issue more carefully and found that the reason for the discrepancy is that Eq. (24) is valid only in a finite range of α_2 , restricted on both sides, and the width of this range turns out to be vanishingly small for $\alpha_1 \sim 0.5 - 0.8$ used by MS.

Specifically, Eq. (19) is obtained under three assumptions:

- that the T -dependence of the bosonic mass can be neglected and the bosonic propagator can be

evaluated at $T = 0$ – this is justified if $m \approx 4\pi m^* v^2 \alpha_2 \gg T_p^{\gamma=1/3}$;

- that typical vk are small compared to m , i.e., $D_b(k)$ can be approximated by its small k form $D_b = v^2 k^2 / (8\pi m)$;
- that typical k are small compared to k_F .

We verified that the first assumption is well satisfied for all $\alpha_1 < 1$ and arbitrary α_2 and is not the subject of concern.

To verify the second assumption we note that typical k leading to (24) are of order $(mk_F \Omega_n / v^2)^{1/3}$, and typical $\Omega_m \sim T_p^{\gamma=1/3}$. Substituting the numbers, we find that for typical k

$$\frac{vk}{m} \sim 2\alpha_1 n^{1/3} \quad (25)$$

where $n \geq 1$ is a number of a Matsubara frequency (typical $n = O(1)$). The condition $vk \ll m$ is then satisfied when α_1 is small enough. There is no dependence on α_2 in this equation, hence for sufficiently small α_1 the condition $vk < m$ is satisfied for all α_2 .

The third condition is satisfied at small α_2 but breaks out at larger α_2 . Indeed, for typical k ,

$$\frac{k}{k_F} \sim 27\alpha_2 n^{1/3} \quad (26)$$

The condition $k/k_F \ll 1$ is satisfied when the r.h.s. of (26) is small.

A. crossover at “large” α_2

The large numerical prefactor in (26) implies that Eq. (24) becomes invalid beginning from quite small $\alpha_2 \sim 10^{-2}$. Once typical k become larger than k_F , $\lambda(\Omega_n)$ has to be re-evaluated because the momentum integral in (19) only extends up to k_F . We assume and then verify that in this situation the Landau damping term Ω_n/k is larger than $D_b(k)$ for all $k < k_F$ and for Ω_m comparable to the actual T_p , which differs from $T_p^{\gamma=1/3}$ in Eq. (24). Neglecting $D_b(k)$ in (19) we obtain in this situation

$$\lambda(\Omega_n) = \frac{\Omega_0^{\gamma=1}}{|\Omega_n|} \quad (27)$$

where $\Omega_0^{\gamma=1} = 4E_F/(3\pi)$. Observe that $\Omega_0^{\gamma=1}$ does not depend on α_2 , in distinction to $\Omega_0^{\gamma=1/3}$ in Eq. (22).

This form of $\lambda(\Omega_n)$ corresponds to the γ -model with $\gamma = 1$. T_p in $\gamma = 1$ model has been obtained in^{8,12}:

$$T_p^{\gamma=1} = 0.254\Omega_0^{\gamma=1} = 0.108E_F. \quad (28)$$

This should be the actual T_p in the MS model at large α_2 . Comparing this $T_p^{\gamma=1}$ with $T_p^{\gamma=1/3}$ from Eq. (24), we

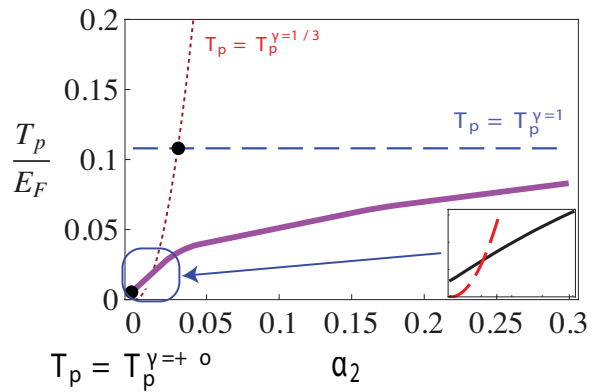


FIG. 4: The interplay between T_p in the MS model and in the γ -model with the pairing kernel $\lambda(\Omega_n) \propto 1/\Omega_n^\gamma$. There is a very tiny range near $\alpha_2 \sim 0.01$ where T_p in the MS model is the same as in $\gamma = 1/3$ model: $T_p = T_p^{\gamma=1/3} = 119E_F\alpha_2^2$. At larger α_2 , the MS model becomes equivalent to the γ model with varying $\gamma > 1/3$. The value of γ increases with α_2 and approaches $\gamma = 1$ at large α_2 . T_p in this regime deviates from α_2^2 dependence of $T_p^{\gamma=1/3}$ and eventually saturates at $T_p = T_p^{\gamma=1} = 0.108E_F$. At smaller α_2 , the MS model becomes equivalent to the γ model with varying $\gamma < 1/3$. T_p in this regime again deviates from α_2^2 dependence of $T_p^{\gamma=1/3}$ and tends to a non-zero value at a magnetic QCP, where $\alpha_2 = 0$. In this limit, the MS model becomes equivalent to the γ -model with $\gamma = 0+$ ($\lambda(\Omega_n) \propto \log \Omega_n$), and $T_p = T_p^{\gamma=0+} \approx 1.8 \frac{E_F}{\alpha_1} e^{-\frac{2}{2\sqrt{\alpha_1}}}$.

clearly see the difference: while $T_p^{\gamma=1/3}$ scales as α_2^2 , the actual T_p saturates at large α_2 .

In the crossover regime, the coupling $\lambda(\Omega_n)$ and the pairing instability temperature T_p should interpolate between $\gamma = 1/3$ and $\gamma = 1$ behavior. The two temperatures $T_p^{\gamma=1/3}$ and $T_p^{\gamma=1}$ cross at $\alpha_2 \sim 0.03$, and the crossover should be around these α_2 . We show the crossover in Fig.4. Note that $\alpha_2 \sim 0.03$ is consistent with our earlier estimate of $\alpha_2 \sim 10^{-2}$ at which typical k becomes comparable to k_F .

To understand the system behavior in the crossover regime, we computed $\lambda(\Omega_n)$ for several α_2 and found that for each given α_2 , $\lambda(\Omega_n)$ can be well fitted over a wide frequency range by $\Omega_n^{-\gamma}$ form, where γ changes between $1/3$ and 1 when α_2 increases. In other words, for a given α_2 , the MS model is equivalent to a γ -model with a particular exponent γ . In Figs. 5 and 6, we plot $\lambda(\Omega_n)$ vs the number of the Matsubara frequency, and the actual T_p as a function of α_1 for $\alpha_2 = 0.02$ and $\alpha_2 = 0.06$. The best fits to γ -model corresponds to $\gamma = 0.6$, $\Omega_0^{\gamma=0.6} = 0.04$, and $\gamma = 0.7$, $\Omega_0^{\gamma=0.7} = 0.11$, respectively. The dashed lines in the figures for T_p are the values of the pairing instability temperature in the γ -model (Ref.¹²): $T_p^{\gamma=0.6} \approx 0.5\Omega_0^{\gamma=0.6} = 0.02E_F$ and $T_p^{\gamma=0.7} \approx 0.38\Omega_0^{\gamma=0.7} = 0.042E_F$. We see that the agreement is nearly perfect, although for $\alpha_2 = 0.02$, there is some residual dependence of T_p on α_1 which is not

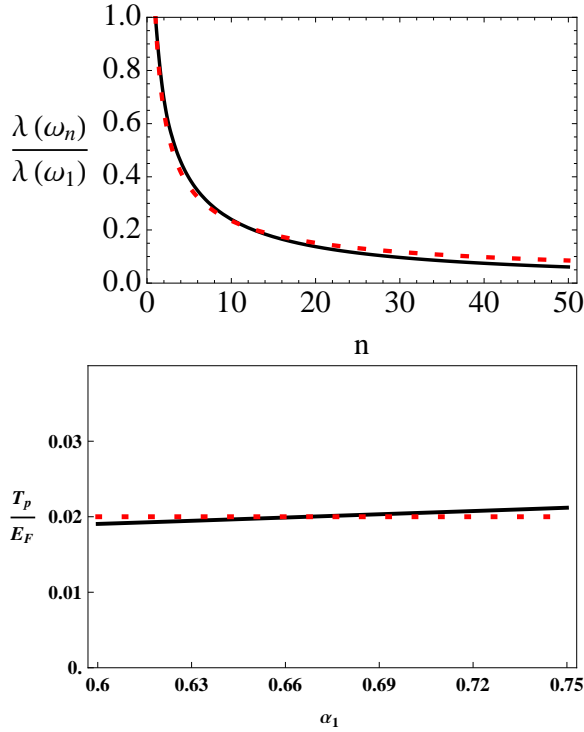


FIG. 5: Solid lines: the dimensionless pairing kernel $\lambda(\Omega_n)$ (panel (a)) for $\alpha_1^2 = 0.32$, and the critical temperature T_p vs the coupling α_1 (panel (b)) at $\alpha_2 = 0.02$ (α_2 measures the distance to an antiferromagnetic QCP). The dashed (red) line in panel (a) is $\lambda(\Omega_m) = (\Omega_0^\gamma/\Omega_n)^\gamma$. The best fit corresponds to $\gamma = 0.6$ and $\Omega_0^{\gamma=0.6} \approx 0.045E_F$. The dotted (red) line in panel (b) is T_p in the γ model for $\gamma = 0.6$: $T_p^{\gamma=0.6} \approx 0.5\Omega_0^{\gamma=0.6} = 0.02E_F$. The agreement is quite good, but there is some variation of the actual T_p/E_F with α_1 implying that the value of γ in the fit of $\lambda(\Omega_n)$ by $1/\Omega^\gamma$ slightly varies with α_1 .

present in the γ -model. In Fig. 7 we show the fit to $1/\Omega_n$ from of λ_n and T_p for the limiting case of large α_2 . We see that the actual T_p perfectly matches $T_p^{\gamma=1} = 0.108E_F$, and the ratio T_p/E_F is totally independent on α_1 .

B. crossover at small α_2

We next consider what happens at small α_2 , when typical k are much smaller than k_F . At the first glance, the analogy with $\gamma = 1/3$ model should work in the small α_2 range because all three conditions used in the derivation of Eqs. (21)-(24) are satisfied. If so, T_p should scale as α_2^2 and vanish at $\alpha_2 = 0$, see Eq. (24). This, however, is not the case as is clearly seen from Fig.3 – the actual T_p remains nonzero at $\alpha_2 = 0$.

The reason for this discrepancy is that the validity of the three conditions $m \gg T$, $vk \ll m$, and $k \ll k_F$ in fact only implies that Eq. (24) is self-consistent at small α_2 . However, there may be another contribution to T_p from the range $vk > m$, and if such additional

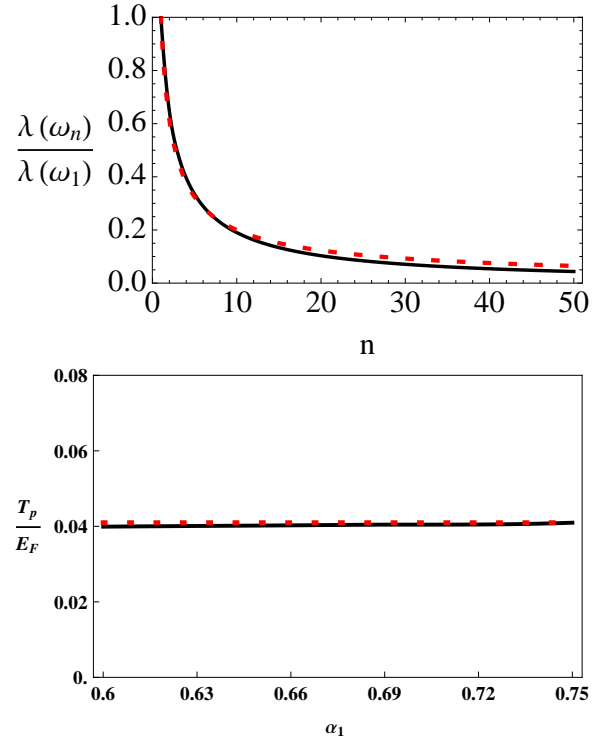


FIG. 6: Same as in Fig. 5 but for a larger $\alpha_2 = 0.06$. The best fit by a power-law (dashed (red) line in panel (a)) now corresponds to $\gamma = 0.7$, and $\Omega_0^{\gamma=0.7} \approx 1.11E_F$. The dotted (red) line is $T_p^{\gamma=0.7} \approx 0.38\Omega_0^{\gamma=0.7} \approx 0.042E_F$. The agreement is quite good, and there is less variation of t_p/E_F than in Fig. 5.

contribution does exist, it may overshadow the contribution from $vk < m$. A good example of such behavior is the case of phonon superconductors at strong coupling^{13,14,16}: McMillan $T_p^{MM} \sim \omega_D e^{-(1+\lambda)/\lambda}$ is self-consistently obtained as a contribution from fermions in a Fermi-liquid region of $\omega < \omega_D$. Yet, there is another contribution to T_p from fermions outside of the Fermi-liquid regime, and at strong coupling ($\lambda \gg 1$) this second contribution overshadows the contribution from the Fermi liquid range and yields Allen-Dynes expression¹⁴ $T_p^{AD} \sim \omega_D \sqrt{\lambda} \gg T_p^{MM}$.

To verify whether the same happens in our case, consider the limit $\alpha_2 = 0$, when T_p given by (24) vanishes. If the actual T_p remains finite at this point, it necessary comes from $vk > m$ simply because $m(T=0) = 0$. Re-evaluating $\alpha(\Omega_n)$ at $\alpha_2 = 0$ and $T = 0$ we obtain $D_b(k) = vk/8$ and

$$\lambda(\Omega_n) = \frac{2\alpha_1}{\pi^2} \left[\sqrt{1 + \frac{|\Omega_n|}{\pi vk_F}} \tanh^{-1} \left(\frac{1}{\sqrt{1 + \frac{|\Omega_n|}{\pi vk_F}}} \right) - 1 \right] \quad (29)$$

At small $\Omega_n \ll vk_F$ this reduces, with logarithmical

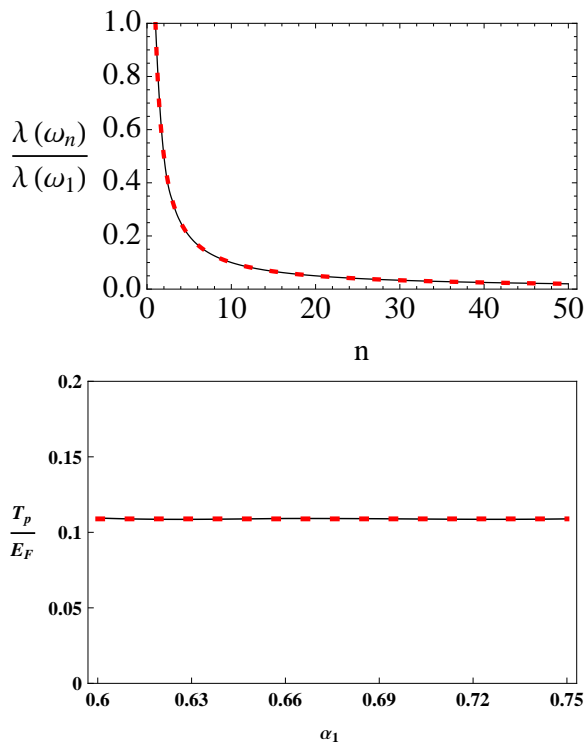


FIG. 7: Dimensionless coupling constant $\lambda_T(\omega_n)$ and critical temperature in the extreme limit of very large $\alpha_2 = 600$. Details are the same as the Fig. 5. The power-law exponent in the fit $\gamma = 1$, $\Omega_0^{\gamma=1} = 4E_F/(3\pi) = 0.424E_F$, and $T_p^{\gamma=1} \approx 0.254\Omega_0^{\gamma=1} \approx 0.108E_F$. This $T_p^{\gamma=1}$ perfectly matches T_p for all α_1 .

accuracy, to

$$\lambda(\Omega_n) = \frac{\alpha_1}{\pi^2} \log \frac{4\pi k_F v}{e^2 |\Omega_n|} = \frac{\alpha_1}{\pi^2} \log \left(\frac{\Omega_0^{\gamma=0+}}{\Omega_n} \right),$$

$$\text{where } \Omega_0^{\gamma=0+} = \frac{8\pi E_F}{e^2 \alpha_1} \quad (30)$$

The model with such $\lambda(\Omega_n)$ is again equivalent to the γ -model, but with $\gamma = 0+$. The $\gamma = 0+$ model with logarithmical kernel has been analysed by Son⁷ and others.^{8,11,19} It *does have* a pairing instability at a non-zero temperature, i.e., the actual T_p does not vanish at $\alpha_2 = 0$, in distinction to Eq. (24). For $\alpha_1 = 0.6$, we found $T_p^{\gamma=0+} \sim 0.005E_F$. This obviously implies that Eq. (24) is valid only in limited range of α_2 , bounded from both ends. Furthermore, comparing this $T_p^{\gamma=0+} \sim 0.005E_F$ with $T_p^{\gamma=1/3}$ from Eq. (24), we find that they become comparable at the same $\alpha_2 \sim 10^{-2}$, where $T_p^{\gamma=1/3}$ becomes comparable to $T_p^{\gamma=1}$. As the consequence, the width of the range where Eq. (24) is valid turns out to be vanishingly small number-wise, although parameter-wise it is $O(1)$. This explains why the actual T_p is so different from $T_p^{\gamma=1/3}$ (see Fig. 3).

We will discuss the form of $T_p^{\gamma=0+}$ in more detail in the next section and here only note that the total T_p in

the MS model is the sum of contributions from $vk > m$ and $vk < m$, i.e., $T_p \sim T_p^{\gamma=0+} + T_p^{\gamma=1/3}$. In the crossover range where $T_p^{\gamma=0+}$ and $T_p^{\gamma=1/3}$ are comparable, the MS model is most likely again fitted by the γ -model with varying γ between 0 and 1/3 (i.e., by different γ for different α_2). However, the width of the crossover range at small α_2 is narrow, and we didn't attempt to fit the data at the smallest α_2 by the γ -model with $0 < \gamma < 1/3$.

IV. THE MS MODEL AT THE SDW QCP – THE EQUIVALENCE WITH COLOR SUPERCONDUCTIVITY

The model with the logarithmical pairing kernel, as in Eq. (30), is most known as a model for color superconductivity of quarks due to the exchange by gluons. For small ω_n , the fermionic self-energy for logarithmical $\lambda(\Omega_n)$ given by (30) is

$$\Sigma(\omega_n) = \int_0^\omega d\omega' \lambda(\omega') = g\omega \log \left(\frac{\Omega_0^{\gamma=0+}}{\omega_n} \right). \quad (31)$$

To shorten notations, we define $g = \alpha_1/\pi^2$. The pairing kernel at small frequencies is $\lambda(\Omega_m) = g \log \left(\frac{\Omega_0^{\gamma=0+}}{\omega_n} \right)$.

The equation for the pairing vertex is, to the logarithmical accuracy,

$$\Phi(\omega) = \frac{g}{2} \int_{T_p^{\gamma=0+}}^{\Omega_0^{\gamma=0+}} d\omega' \frac{\Phi(\omega') \log \left(\frac{\Omega_0^{\gamma=0+}}{|\omega' - \omega|} \right) + \log \left(\frac{\Omega_0^{\gamma=0+}}{|\omega' + \omega|} \right)}{1 + g \log \left(\frac{\Omega_0^{\gamma=0+}}{\omega'} \right)}$$

$$= g \int_{T_c}^{\Omega_0^{\gamma=0+}} d\omega' \frac{\Phi(\omega') \log \left(\frac{\Omega_0^{\gamma=0+}}{\sqrt{|\omega'^2 - \omega^2|}} \right)}{1 + g \log \left(\frac{\Omega_0^{\gamma=0+}}{\omega'} \right)}. \quad (32)$$

The logarithm in the denominator is the contribution from the self-energy, Eq. (31). At small coupling, $g \ll 1$, which we only consider, the self-energy can be dropped, and the condition that the solution of (32) exists reduces to $g \log^2(\Omega_0^{\gamma=0+}/T_p^{\gamma=0+}) = O(1)$, i.e., $\log T_c \propto 1/\sqrt{g}$. A more accurate solution was obtained by Son⁷:

$$T_p^{\gamma=0+} = c \Omega_0^{\gamma=0+} e^{-\frac{\pi}{2\sqrt{g}}} = \bar{c} \frac{E_F}{\alpha_1} e^{-\frac{\pi^2}{2\sqrt{\alpha_1}}} \quad (33)$$

where c and $\bar{c} = 8\pi c/e^2$ are numbers $O(1)$. The smaller is α_1 , the smaller is $T_p^{\gamma=0+}$ and the smaller is the crossover scale below which the actual T_p deviates from $T_p^{\gamma=1/3}$.

To obtain the prefactor c in (33), one has to go beyond the leading logarithmical accuracy and include (i) \sqrt{g} corrections to the argument of the exponent and (ii) the actual soft high-energy cutoff in the full expression for $\lambda(\Omega_n)$, see Eq. (29). The \sqrt{g} corrections to the argument of the exponent come from fermionic self-energy. These corrections have been computed analytically in Ref.¹¹, and the result is that the fermionic self-energy

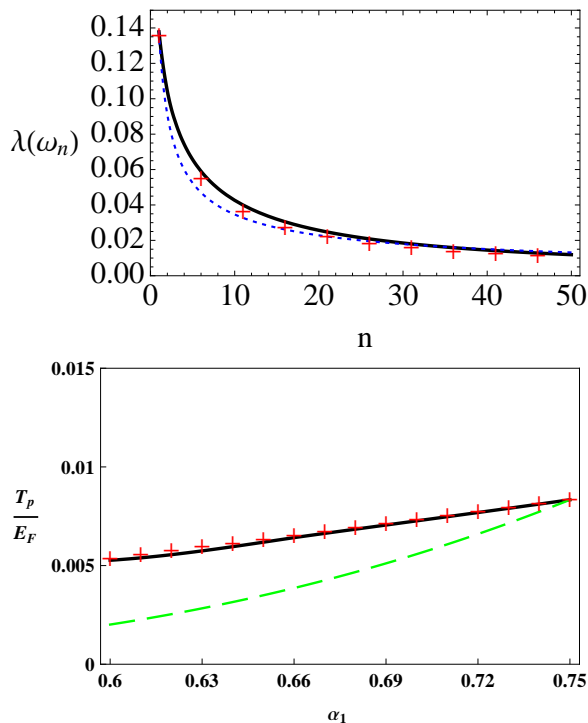


FIG. 8: Solid lines: the pairing kernel $\lambda(\Omega_n)$ (panel (a)) and the critical temperature T_p in the MS model at the critical point, $\alpha_2 = 0$ (panel (b)). In panel (a) we set $\alpha_1^2 = 0.32$. The crossed (red) line in panel (a) is the fit to $\lambda(\Omega_n) = (\alpha_1/\pi^2) \log(\Omega_0^{\gamma=0+}/\Omega_n)$ with $\Omega_0^{\gamma=0+} = \frac{8\pi E_F}{e^2 \alpha_1}$ (see Eq. (30)). For comparison, the dotted (blue) line is the fit by a power-law with $\gamma = 0.6$. Obviously, the fit by $\gamma = 0+$ form is much better. The crossed (red) line in panel (b) corresponds to $T_p^{\gamma=0+} \approx 1.8 \frac{E_F}{\alpha_1} e^{-\frac{\pi^2}{2\sqrt{\alpha_1}}}$. The fit is almost perfect (solid and dashed lines are virtually indistinguishable). For comparison, we also show the fit to the BCS behavior $T_p^{BCS} \propto 1/\alpha_1 e^{-\pi/2\alpha_1}$ (the dashed (green) line), adjusting the prefactor to match T_p at $\alpha_1 = 0.75$. We clearly see that T_p in the MS model follows $T_p^{\gamma=0+}$ rather than the BCS form.

contributes the universal factor $e^{(\pi^2+4)/8} = 0.177$ to c . The effect of a soft high-energy cutoff depends on how the logarithmical form of $\lambda(\Omega_n)$ is cut and is model-dependent.

To the best of our knowledge, the non-trivial dependence of $T_p^{\gamma=0+}$ on the coupling $g = \alpha_1/\pi^2$ has not been verified numerically. The equivalence between the MS model at $\alpha_2 = 0$ and the γ model with $\gamma = 0+$ allows us to do this and also to determine the value of the prefactor in our case. In Fig. (8) we show the fit of $\lambda(\Omega_n)$ for $\alpha_2 = 0$ to $1/\Omega_n$ dependence (which is almost perfect) and the numerical results for T_p/E_F vs α_1 . We fitted the data by Eq. (33), i.e. by $(1/\alpha_1) e^{-\pi^2/(2\sqrt{\alpha_1})}$ dependence on α_1 , and, for comparison, by BCS dependence. We see that the fit by Eq. (33) is nearly perfect. We emphasize that $1/\sqrt{\alpha_1}$ dependence in the exponent and the presence of $1/\alpha_1$ in the overall factor are both relevant to the success of the fit. We view this agreement as the solid

verification of Son's formula for color superconductivity. From the fit we also determined $c \approx 0.037$, and $\bar{c} \approx 1.8$.

V. CONCLUSIONS

To conclude, in this paper we analysed the onset temperature T_p for the pairing in cuprate superconductors at small doping, when tendency towards antiferromagnetism is strong. We considered the model, introduced by Moon and Sachdev, which assumes that the Fermi surface retains pocket-like form, same as in an antiferromagnetically ordered state, even when long-range antiferromagnetic order disappears. Within this model, the pairing between fermions is mediated by a gauge boson, whose propagator remains massless despite that magnon dispersion acquires a finite gap in the magnetically disordered phase. From the point of view of quantum-critical phenomenon, the pairing problem then remains quantum critical in the sense that the pairing is mediated by a gapless boson, and the same gapless boson that mediates pairing also accounts for the destruction of a Fermi-liquid behavior down to the smallest frequencies.

We related the MS model to the generic γ -model of quantum-critical pairing with the pairing kernel $\lambda(\Omega_n) \propto 1/\Omega_n^\gamma$ and the corresponding normal state self-energy $\Sigma(\omega_n) \propto \omega_n^{1-\gamma}$. We showed that, over some range of parameters, the pairing problem in the MS model in a paramagnetic phase predominantly comes from fermions with momenta $k \ll k_F$, where k_F is the Fermi momentum, and $vk \ll m$, where v is the Fermi velocity, and m is the magnon gap. In this situation, the pairing in the MS model is equivalent to that in the γ -model with $\gamma = 1/3$. We found that T_p scales as α_2^2 , where α_2 is the parameter which measures how far the system moves away from the SDW phase.

On a more careful look, we found that the range of α_2 where the analogy with the $\gamma = 1/3$ model works is bounded at both small and "large" α_2 . At "large" α_2 (which numerically are still quite small), the condition $k \ll k_F$ breaks down. We demonstrated that, in this situation, the MS model becomes equivalent to γ model with varying γ , whose value increases with α_2 and approaches $\gamma = 1$ at large α_2 . In the crossover regime, the actual $T_p(\alpha_2)$ deviates from the α_2^2 dependence and eventually saturates at large α_2 at $T_p \sim 0.1E_F$.

At the smallest α_2 , we found that the analogy with $\gamma = 1/3$ model again breaks down, this time because the contribution to T_p from $vk \ll m$ gets overshadowed by the contribution from $vk \gg m$. In this situation, the MS model becomes equivalent to the γ -model with $\gamma < 1/3$. Finally, at $\alpha_2 = 0$, i.e., at the SDW transition point, the MS model becomes equivalent to the γ model with $\gamma = 0+$, for which $\lambda(\Omega_m) \propto \log \Omega_m$.

The $\gamma = 0+$ model has been studied in the context of color superconductivity and superconductivity near 3D ferro- and antiferromagnetic QCP. The pairing problem with the logarithmical pairing kernel is similar to the

BCS theory in the sense that the fermionic self-energy can be neglected in the leading logarithmic approximation at weak coupling g . However, in distinction to the BCS theory, $\log T_c$ scales not as $1/g$ but as $1/\sqrt{g}$. We used the analogy between the MS and the $\gamma = 0+$ model at small frequencies and the fact that $\lambda(\Omega_n)$ in the MS model does converge at high frequencies (i.e., one does not have to introduce a cutoff), and computed T_p numerically. We explicitly verified the $1/\sqrt{g}$ behavior in the exponent and also verified the $1/g$ dependence of the overall factor for T_p . To the best of our knowledge, this has not been done before.

Overall, our results imply that the MS model is quite

rich. It contains the physics of the quantum-critical pairing in all models with kernels $\lambda(\Omega_n) \propto 1/\Omega_n^\gamma$ and $0 < \gamma \leq 1$. In addition, the MS model taken at the point of the magnetic instability is equivalent to the model for color superconductivity. It is amazing that one can get useful information about color superconductivity by studying the pairing at the antiferromagnetic instability in the cuprates. We thank S. Sachdev, M. Metlitskii and J. Schmalian for the interest to this work and useful comments. This work was supported by NSF DMR-0757145 and the Samsung Scholarship (E.G. Moon) and by NSF-DMR-0906953 (A. V. Ch.)

-
- ¹ for a review, see e.g., Ar. Abanov, A.V. Chubukov, and J. Schmalian, *Adv. Phys.* **52**, 119 (2003).
- ² Ar. Abanov, A. V. Chubukov, and A.M. Finkelstein, *Europhys. Lett.* **54**, 488 (2001).
- ³ P. A. Lee, *Phys. Rev. Lett.* **63**, 680 (1989); J. Polchinski, *Nucl. Phys. B* **422**, 617 (1994); B. L. Altshuler, L. B. Ioffe, and A. J. Millis, *Phys. Rev. B* **50**, 14048 (1994); **52**, 5563 (1995); C.J. Halboth and W. Metzner, *Phys. Rev. Lett.* **85**, 5162 (2000);
- ⁴ H. Yamase and H. Kohno, *J. Phys. Soc. Jpn.* **69**, 332 (2000); **69**, 2151 (2000); V. Oganesyan, S. A. Kivelson, and E. Fradkin, *Phys. Rev. B* **64**, 195109 (2001); A. V. Chubukov, A. M. Finkelstein, R. Haslinger, and D. K. Morr, *Phys. Rev. Lett.* **90**, 077002 (2003); Y.-B. Kim, A. Furusaki, X.-G. Wen, and P. A. Lee, *Phys. Rev. B* **50**, 17917 (1994); H.-Y. Kee and Y.-B. Kim, *Phys. Rev. B* **71**, 184402 (2005); J. Nilsson and A. Castro Neto, *Phys. Rev. B* **72**, 195104 (2005); J. Quintanilla and A. J. Schofield, *Phys. Rev. B* **74**, 115126 (2006); J. Rech, C. Pépin, and A. V. Chubukov, *Phys. Rev. B* **74**, 195126 (2006); L. Dell’Anna and W. Metzner, *PRB* **73**, 045127 (2006); P. Wölfle and A. Rosch, *J. Low Temp. Phys.* **147**, 165 (2007); arXiv:cond-mat/0609343; T. Senthil, *Phys. Rev. B* **78**, 035103 (2008); M. Zacharias, P. Wölfle, and M. Garst, *Phys. Rev. B* **80**, 165116 (2009); S.-S. Lee, *Phys. Rev. B* **80**, 165102 (2009); D. Maslov and A. Chubukov, D.L. Maslov and A.V. Chubukov, *Phys. Rev. B* **81**, 045110 (2010); M. Metlitski and S. Sachdev, arXiv:1001.1153; D. F. Mross, J. McGreevy, H. Liu, and T. Senthil, arXiv:1003.0894; E. Fradkin, S. A. Kivelson, M. J. Lawler, J. P. Eisenstein, and A. P. Mackenzie, arXiv:0910.4166.
- ⁵ E. G. Moon, and S. Sachdev, *Phys. Rev. B* **80**, 035117 (2009).
- ⁶ S. Sachdev, M. A. Metlitski, Y. Qi, and C. Xu, *Phys. Rev. B* **80**, 155129 (2009)
- ⁷ D. T. Son, *Phys. Rev. D* **59**, 094019 (1999)
- ⁸ A. Chubukov, and J. Schmalian, *Phys. Rev. B* **72**, 174520 (2005). The value of T_p in the Appendix C of this paper should be multiplied by 4.
- ⁹ N. E. Bonesteel, I. A. McDonald, and C. Nayak *Phys. Rev. Lett.* **77**, 3009 (1996). The prefactor for T_p reported in this paper is slightly larger than the one in Ref.¹²
- ¹⁰ D. V. Khveshchenko and W. F. Shively, *Phys. Rev. B* **73**, 115104 (2006); A. V. Chubukov and A. M. Tsvelik, *Phys. Rev. B* **76**, 100509 (2007).
- ¹¹ W.E. Brown, J.T. Liu, and H.-C. Ren, *Phys. Rev. D* **61**, 114012 (2000); **62**, 054013 (2000); **62**, 054016 (2000); Q. Wang and D.H. Rischke, *Phys. Rev. D* **65**, 054005 (2002). Similar calculations for a Fermi gas with s -wave attractive interaction have been carried out by L.P. Gorkov and T.K. Melik-Barkhudarov, *Sov. Phys. JETP* **13**, 1018 (1961), and for p -wave pairing by A.V. Chubukov and A. Sokol, *Phys. Rev. B* **49**, 678, 1994. For Kohn-Luttinger problem, the corrections to the exponent have been obtained by D. Efremov, M.S. Marienko, M.A. Baranov, and M. Yu. Kagan, *JETP* **90**, 861 (2000).
- ¹² Ar. Abanov, B. Altshuler, A. Chubukov, and E. Yuzbashyan, unpublished.
- ¹³ See, e.g., F. Marsiglio and J.P. Carbotte, “Electron-Phonon Superconductivity”, in “The Physics of Conventional and Unconventional Superconductors”, edited by K.H. Bennemann and J.B. Ketterson, Springer-Verlag, 2006.
- ¹⁴ P.B. Allen and R.C. Dynes, *Phys. Rev. B* **12**, 905 (1975).
- ¹⁵ For a review of recent works, see e.g., S. Sachdev, arXiv:1002.3823.
- ¹⁶ R. Combescot, *Phys. Rev. B* **51**, 11625 (1995)
- ¹⁷ G.M. Eliashberg, *Sov. Phys. JETP*, **11**, 696 (1960)
- ¹⁸ J. R. Schrieffer, X.-G. Wen, and S.-C. Zhang *Phys. Rev. Lett.* **60**, 944 (1988); V.V.Flambaum, M.Yu.Kuchiev, and O.P.Sushkov, *Physica C227*, 267 (1994); V.I. Belinicher, A.L. Chernyshev, A.V. Dotsenko, and O.P. Sushkov, *Phys. Rev. B* **51**, 6076 (1995).
- ¹⁹ Z. Wang, W. Mao, and K. Bedell, *Phys. Rev. Lett.*, **87**, 257001 (2001). R. Roussev and A.J. Millis, *Phys. Rev. B* **63**, 140504 (2001).
- ²⁰ M. Metlitski and S. Sachdev, unpublished
- ²¹ T.A. Sedrakyan and A.V. Chubukov, arXiv:1002.3824
- ²² A. J. Millis, S. Sachdev, and C. M. Varma, *Phys. Rev. B* **37**, 4975 (1988).
- ²³ Ar. Abanov, A.V. Chubukov, and M. Norman, *Phys. Rev. B* **78**, 220507 (2008).